Study of the interfacial regions in Fe/Cr multilayers

W. Alayo,[a] Miguel Tafur, Y. T. Xing, and E. Baggio-Saitovitch
Centro Brasileiro de Pesquisas Físicas, Rua Dr. Xavier Sigaud 150, Urca, CEP 22290-180, Rio de Janeiro, Brazil

V. P. Nascimento
Instituto Multidisciplinar, Universidade Federal Rural do Rio de Janeiro, Rua Professor Paris, s/n Centro, CEP 26221-150, Nova Iguaçu, Rio de Janeiro, Brazil

A. D. Alvarenga
Instituto Nacional de Metrologia, Normalização e Qualidade Industrial, Av. Nossa Senhora das Graças 50, Duque de Caxias, Rio de Janeiro, 25250-020, Brazil

(Received 9 May 2007; accepted 7 August 2007; published online 4 October 2007)

The magnetism at the interfacial regions of the $[Fe(50\ Å)/Cr(27\ Å)]_{20}$ antiferromagnetic coupled multilayer was studied using the x-ray magnetic circular dichroism (XMCD) technique. Two experimental approaches were used to reach the interface regions. In the first one, multilayers of the same type, deposited with the Cr capping layer with different thicknesses of 30, 20, 10, and 5 Å, were analyzed and we obtained a magnetic depth profile without removing the layers. In the second approach, the layers of the sample were thinned by several *in situ* sputtering cycles with Ar^+ ions, followed by XMCD analysis. We found a strong reduction of the Fe spin magnetic moments in the sputtered sample, which was caused by the erosion of the layers. On the contrary the noneroded samples kept the Fe bulk moment values. The observation of Cr XMCD signal evidenced an induced moment on Cr antiparallel to the Fe moments. © *2007 American Institute of Physics*. [DOI: 10.1063/1.2786023]

I. INTRODUCTION

Multilayer films consisting of magnetic metals separated by nonmagnetic materials are nowadays a subject of great research, because of their important technological applications and the fundamental physical phenomena that occur in these systems. Some of these phenomena are indirect exchange coupling between magnetic metals via nonmagnetic spacer layers,[1,2] and giant magnetoresistance.[3] Other important phenomena occur at the interfaces, such as induced magnetic moments on atoms in normally nonmagnetic metals, in proximity to magnetic metals. The Fe/Cr multilayers were studied extensively since a decade ago. A theoretical calculation of the distribution of the magnetic moments on Fe/Cr superlattices with perfect or diffuse interfaces showed that the interfacial moments of Fe (Cr) are reduced (increased) if compared to their bulk values.[4] A previous experimental study, using the x-ray magnetic circular dichroism (XMCD) technique, found that the Cr moments are antiparallel to the Fe moments and that for a Cr thickness of 1 ML the average moment was $-0.7\mu_B$/atom.[5] Perturbed angular correlation studies were done in order to determine the magnetic state of epitaxially grown Fe/Cr(100) multilayers[6] and revealed that the magnetization in the Cr layers is oriented perpendicularly to the magnetization of the neighboring Fe layers, and a bulklike antiferromagnetic ordering in Cr is observed above a critical Cr thickness of about 5 nm. Those studies are extensive; however, there are no reports focusing on the orbital and spin moment configuration separately.

The XMCD technique, on the other hand, is a very-well established tool for investigating the magnetism of thin films and multilayers. It is an element-specific method, based on the polarization state dependence of the absorption of circularly polarized synchrotron radiation. For the 3*d* metals, the absorption edges of interest fall at the soft x-ray energy region, where the probing depth is a few nanometers, suitable for the investigations of surfaces and interfaces.

Here the interfacial magnetism of the Fe/Cr multilayer was investigated by the XMCD technique. Spectra were measured at the Fe and Cr $L_{2,3}$ absorption edges and the sum rules[7,8] were applied to obtain the values of the Fe orbital and spin moments. The multilayers were prepared by dc-magnetron sputtering and characterized by x-ray diffraction, magnetoresistance, and magnetization measurements at CBPF. We selected the $[Fe(50\ Å)/Cr(27\ Å)]_{20}$ antiferromagnetic coupled multilayer for the XMCD studies, which were performed at the Synchrotron Light National Laboratory (LNLS), Campinas, Brazil, using the spherical grating monochromator beamline (D08A-SGM).

II. EXPERIMENTAL PROCEDURE

The multilayer samples were prepared using a dc-magnetron sputtering system model ATC-2400 from AJA International. They have the configuration $[Fe(50\ Å)/Cr(t_{Cr})]_{20}$ deposited onto a Cr (30 Å) buffer layer over a Si(100) substrate and covered by a protective Cr (30 Å) capping layer. The base pressure of the deposition chamber was around 5×10^{-8} Torr. The argon pressure (working pressure) during the deposition was kept at 2 mTorr and the deposition rate was 0.58 Å/s for Cr and was 1.32 Å/s for Fe. The Cr

[a]Author to whom correspondence should be addressed. Electronic mail: walayo@cbpf.br

layer thickness was varied around the second peak (t =23,25,27,29 Å) of the saturation magnetoresistance versus Cr thickness curve, as reported on the literature,[1] while the Fe layer thickness was kept constant. All samples were deposited at room temperature.

The magnetotransport characterization was performed by magnetoresistance measurements at room temperature, with the current-in-plane (CIP) geometry, in an applied magnetic field parallel to the sample plane and perpendicular to the current. The resulting data for the sample with a Cr layer thickness of 27 Å showed an antiferromagnetic coupling, and this sample was selected to be studied. The structural characterization was performed by x-ray diffraction at room temperature. Magnetization curves (M-H) also at room temperature were registered using a superconducting quantum interference device (SQUID) magnetometer, in a maximum field of 10 kOe oriented at angles of 0° and 45° with the sample plane in order to estimate the magnetization direction with respect to the sample plane in the XMCD experiments. After selecting the sample for the XMCD studies, we reproduced samples of composition $[\mathrm{Fe}(50\ \text{Å})/\mathrm{Cr}(27\ \text{Å})]_{19}/\mathrm{Fe}(50\ \text{Å})/\mathrm{Cr}(t)$ with t=30, 20, 10, and 5 Å, varying the Cr capping layer thickness in order to reach several depths of the multilayer.

The samples were transported in a small vacuum box to the LNLS facility for the XMCD experiments at the SGM beamline. Circularly polarized light (70%) from a dipole was selected by a slit, and the incoming flux was measured using the current from a gold grid, placed before the chamber, for normalization purposes. Inside the high vacuum chamber (5×10^{-8} Torr), the sample was mounted at an angle of 45° to the incident beam direction. A constant magnetic field of 2 kOe oriented parallel to the x-ray beam direction was provided by a permanent magnet placed behind the tilted sample holder: in this way the multilayer plane was oriented at 45° to the field lines. An electric bias ring was located in front of the sample with an applied voltage of +400 V to capture emitted electrons in order to avoid reabsorption. This vacuum chamber was also equipped with an argon inlet for *in situ* sputtering of the sample. A profile of the x-ray beam was performed after each sputtering cycle in the following way: a step motor moved the slit through the beam, while the intensity was recorded at a diode and monitored by the computer. The resulting curve intensity versus step allows for the choice of the correct position for the slit, at 1/3 of the maximum intensity below the orbit, which is 70% circularly polarized. The sample x-ray absorption spectra (XAS) were recorded by measuring the drain current using a Keithley electrometer.

The multilayers with different thicknesses of the capping layer were measured without *in situ* sputtering of the samples. Only the sample $\mathrm{Si}(100)/[\mathrm{Fe}(30\ \text{Å})/\mathrm{Cr}(27\ \text{Å})]_{20}/\mathrm{Cr}(30\ \text{Å})$ was eroded by several sputtering cycles to obtain an absorption-depth profile of the film. After each cycle, several pairs of XAS for each element were collected. Thus, the spectra were obtained as a function of the sputtering time, which was later converted to sputtered depth by the determination of the sputtering rate (depth divided by time) using an auxiliary experiment.[9] Each pair was obtained with two opposite applied magnetic field directions. The direction of the applied magnetic field was switched by rotating the magnet. The XMCD spectra are the difference between two XAS taken with opposite circular polarizations. This is equivalent to fix the polarization state and reversing the external magnetic field direction. By application of the sum rules to the experimental XMCD spectra, the orbital and spin magnetic moments could be determined separately.

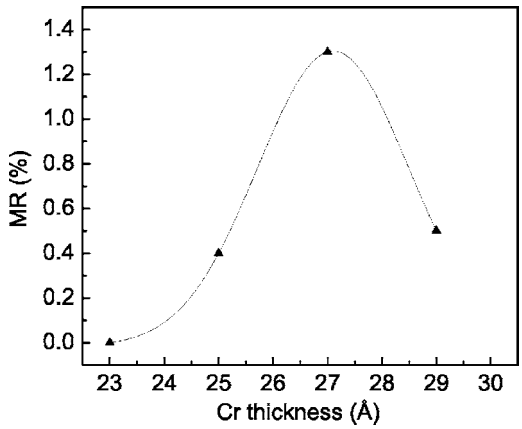

FIG. 1. The magnetoresistance vs Cr layer thickness dependence around the second peak of the MR of the $[\mathrm{Fe}(50\ \text{Å})/\mathrm{Cr}(27\ \text{Å})]_{20}$ multilayer at room temperature.

The data analysis was performed in the following way: all XAS were normalized by the absorption signal to the incoming flux, a linear background was subtracted, and the XMCD spectra were obtained. Each pair of XAS was averaged to obtain an isotropic XAS, which is a good approximation for the isotropic absorption with linear polarized light,[10] and this was used to calibrate the absorption-depth profile. The application of the sum rules to the experimental data is necessary to remove the contribution of the excitations into the continuum, which is modeled as a step function to be subtracted from the isotropic XAS. This procedure will be detailed in the next section.

III. RESULTS AND DISCUSSION

The magnetoresistance versus Cr layer thickness dependence around the second peak is given in Fig. 1. This picture shows that the maximum magnetoresistance value occurs at the Cr thickness of 27 Å. For this reason, one can be confident that for this value of Cr thickness, the coupling between the Fe layers is antiferromagnetic.

The $[\mathrm{Fe}(50\ \text{Å})/\mathrm{Cr}(27\ \text{Å})]_{20}$ antiferromagnetic coupled multilayer was the sample chosen for the study proposed here. An x-ray diffraction scan, at low and high (inserted graphic) angle regions of the $[\mathrm{Fe}(50\ \text{Å})/\mathrm{Cr}(27\ \text{Å})]_{20}$ film, is shown in Fig. 2. In the low angle scan, three superlattice peaks are well identified, indicating the layered structure of the sample. In the high angle scan, the Fe/Cr superlattice and Si(100) substrate reflections are identified at 44.6° and 69°, respectively, speaking for a growth with texture [110]. The complete saturation of the $[\mathrm{Fe}(50\ \text{Å})/\mathrm{Cr}(27\ \text{Å})]_{20}$ multilayer was not reached up to a field of 10 kOe, applied at an angle of 45° with the sample plane, as shown in the hysteresis loop of Fig. 3. However, it is not difficult to calculate the field

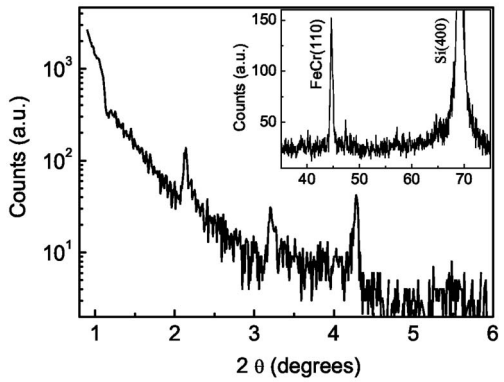

FIG. 2. X-ray diffraction result for the $[Fe(50\ Å)/Cr(27\ Å)]_{20}$ multilayer.

necessary to saturate the sample under this condition, considering that the main contribution to the enhancement of the saturation field as the external field direction apart from the easy plane comes from the shape anisotropy. Using the geometry for thin films, the bulk volume magnetization of Fe (1700 emu/cm^3) and the field (about 1 kOe) necessary to saturate the sample in plane (curve not shown here); the saturation field calculated for an orientation of 45° with the sample plane is about 16 kOe. Furthermore, using the equilibrium condition of the magnetization (considering the shape and magnetocrystalline anisotropies and the Zeeman energy), one can estimate that when a field of 2 kOe is oriented 45° out of the sample plane, the magnetization is oriented uniformly 4° out of plane. Thus, the angle between the incident photon and the sample magnetization is about 41°, which will be used in Eqs. (3) and (4).

The XMCD analysis of the samples $[Fe(50\ Å)/Cr(27\ Å)]_{19}/Fe(50\ Å)/Cr(t)$ will be presented and discussed below. A representative figure of the multilayer is displayed in Fig. 4(a) in order to show the explored depths of the films with different capping Cr layer thickness, denoted by t in the figure. The escape depth of the electrons[15] is assumed to be around 60 Å and is denoted by e. Thus, the Cr capping layer thickness and the escape depth give the depths obtained in the sample. Figure 4(b) displays the absorption-depth profile given by the intensities of the absorptions at the Fe and Cr L_3 peaks of the respective isotropic spectra. In this depth profile we observe an increase of the Fe absorption and a decrease of the Cr as the capping layer is decreased. This is expected due to the amount of material present at the indicated depths that contribute to the absorption.

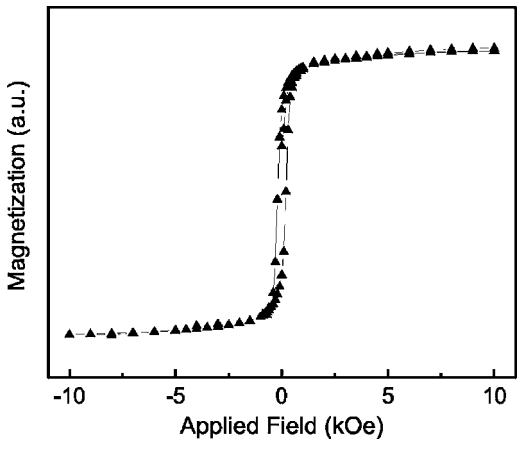

FIG. 3. Magnetization loop performed in an applied magnetic field doing an angle of 45° with the sample plane, at room temperature.

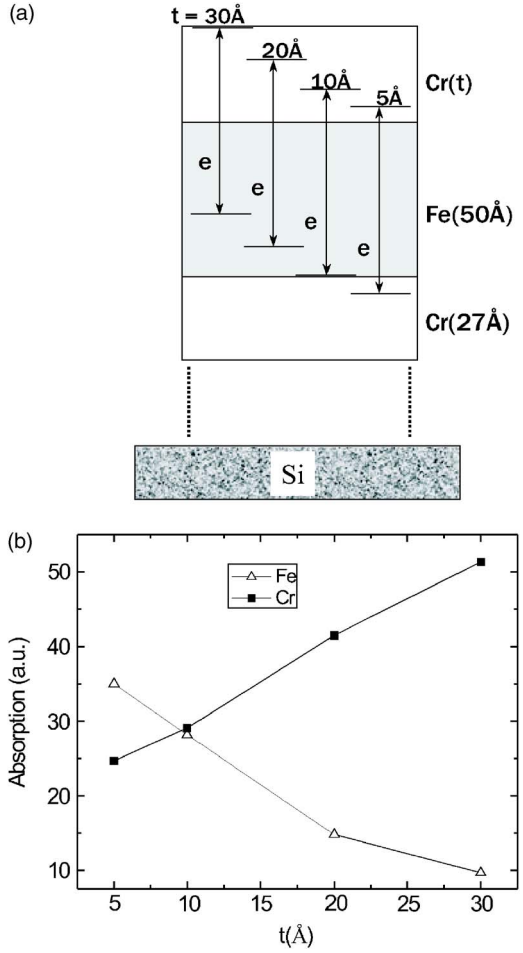

FIG. 4. (Color online) (a) Scheme of the multilayers showing the depths analyzed, given by the Cr capping layer thickness (t) and the escape depth (e=60 Å) of the electrons. (b) Absorption-depth profile of the $[Fe(50\ Å)/Cr(27\ Å)]_{19}/Fe(50\ Å)/Cr(t)$ multilayer.

The representative normalized XAS and XMCD spectra at the Fe and Cr $L_{2,3}$ edges of the multilayer with t=20 Å are displayed in Figs. 5 and 6, respectively. In Fig. 7 are shown only the Cr XMCD signals for the samples with t=10 and 5 Å. These Cr dichroism effects are small compared to the Fe dichroism and reveal an induced magnetic moment with opposite onsets in sign, marked by the arrows in Figs. 4 and 5, indicating an antiparallel alignment between Fe and Cr moments, in agreement with a previous work.[11] This is attributed to a considerable hybridization of Fe and Cr d orbitals near the interface. In the sample with t=30 Å, a Cr dichroism were not clearly observed because the Cr XMCD signals were very noisy and had a very low intensity and it is not shown here. This is attributed to the fact that only the Cr atoms, which have Fe as first neighbors, can contribute to the Cr XMCD signal. This is due to the fact that within the bulk of the Cr layers, essentially no Cr XMCD signal is expected because the antiferromagnetic arrangement of Cr moments leaves no net moment parallel to the applied magnetic field,

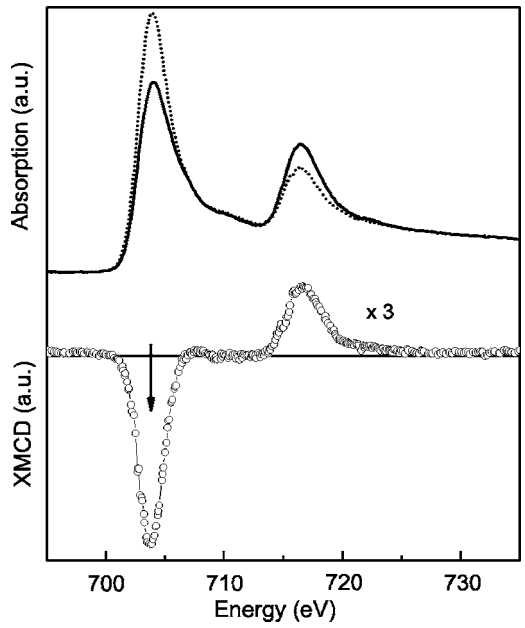

FIG. 5. Normalized XAS and XMCD spectra for Fe in the $[Fe(50\ Å)/Cr(27\ Å)]_{19}/Fe(50\ Å)/Cr(20\ Å)$ multilayer.

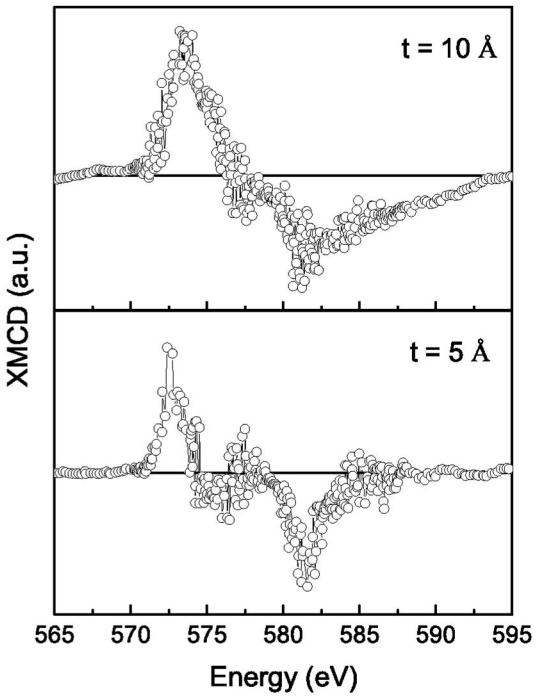

FIG. 7. XMCD spectra for Cr in $[Fe(50\ Å)/Cr(27\ Å)]_{19}/Fe(50\ Å)/Cr(t)$ for $t=5$ and 10 Å.

which in turn is much too small to produce a measurable polarization in bulk Cr. Concerning the determination of the Cr magnetic moments, the sum rules cannot be applied in the case of Cr and in general in the case of the early $3d$ transition metals,[14,16] since the spin-orbit splitting of the initial $2p$ core levels is very small and it leads to a remixing of spin components of the $2p_{3/2}$ and $2p_{1/2}$ states. Here we did not calculate the Cr magnetic moments, but just give evidences of the induced magnetism via the XMCD spectra.

In the case of Fe, the analysis via the sum rules yields magnetic moment values similar to the Fe bulk. The orbital and spin sum rules allow for the quantitative separation of the values of the orbital $m_l=-\mu_B\langle L_z\rangle/\hbar$ and spin $m_s=-2\mu_B\langle S_z\rangle/\hbar$ magnetic moments, where $\langle L_z\rangle e\langle S_z\rangle$ are the expectation values of the orbital and spin operators, respectively. For excitation into d orbitals, the magnetic moments can be determined from the equations below according to Refs. 9 and 10,

$$\frac{A_3-2A_2}{A_{\rm iso}}=\frac{2}{3n_h}\langle S_z\rangle+\frac{7}{3n_h}\langle T_z\rangle, \tag{1}$$

$$\frac{A_3+A_2}{A_{\rm iso}}=\frac{\langle L_z\rangle}{2n_h}, \tag{2}$$

where A_3 and A_2 are the areas under the L_3 and L_2 XMCD spectra, respectively, $A_{\rm iso}$ is the isotropic area, n_h is the number of valence holes, and $\langle T_z\rangle$ is the magnetic dipole term. The photoelectron excitations into the continuum states are modeled as a two-step function[12] and here, this function is given by $a_0(x)=h_3/(1+e^{-k_3(x-x_3)})+h_2/(1+e^{-k_2(x-x_2)})$. The steps occur at the energy positions of the $L_2(x_2)$ and $L_3(x_3)$ peaks, and k_2 and k_3 are the linewidths at the half-height of the L_2 and L_3, respectively. The height of the step $L_2(L_3)$ is 1/3(2/3) of the intensity h of the last 15 eV of the isotropic XAS. After subtracting the step function from the isotropic XAS, the isotropic area $A_{\rm iso}$ is obtained by integration of the resulting XAS.

The sum rule of Eq. (1) allows for the determination of the sum of the spin magnetic moment m_s and the dipole magnetic moment m_T, termed the effective spin magnetic moment $m_s^{\rm eff}$. In the present work only $m_s^{\rm eff}$ could be determined because a magnetic field oriented at 45° to the normal of the sample plane was used; under this condition it is not possible to obtain the value of the dipolar contribution separately, and thus only the $m_s^{\rm eff}$ values were quoted. The orbital

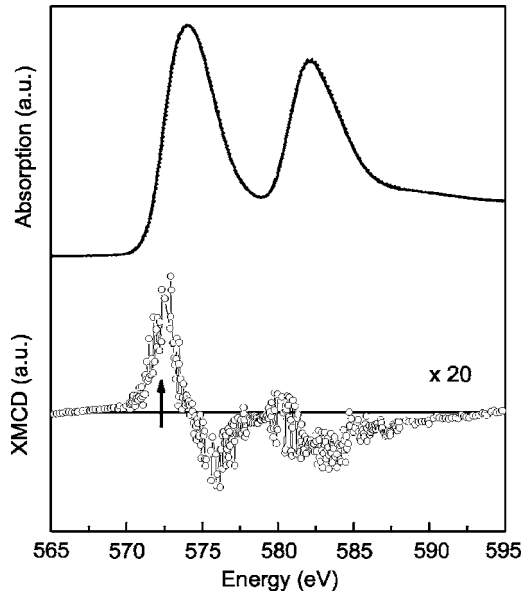

FIG. 6. Normalized XAS and XMCD spectra for Cr in the $[Fe(50\ Å)/Cr(27\ Å)]_{19}/Fe(50\ Å)/Cr(20\ Å)$ multilayer.

TABLE I. Spin and orbital magnetic moments for Fe in $[Fe(50\ Å)/Cr(27\ Å)]_{19}/Fe(50\ Å)/Cr(t)$ multilayers with several thicknesses of the top Cr layer.

Top Cr layer thickness t (Å)	m_s^{eff} (μ_B/atom)	m_l (μ_B/atom)
30	1.95	0.14
20	1.91	0.20
10	2.00	0.21
5	2.12	0.24

and effective spin magnetic moment can be determined directly from the experimental data after rearranging the sum rules, as in Ref. 13:

$$m_s^{\text{eff}} = -\frac{n_h}{P_c \cos\theta}\frac{A_3 - 2A_2}{A_{\text{iso}}}, \tag{3}$$

$$m_l = -\frac{2n_h}{3P_c \cos\theta}\frac{A_3 + A_2}{A_{iso}}, \tag{4}$$

here θ (41°) is the angle between the magnetization and the wave vector of the incident photon; P_c is the circular polarization degree of the beam, here P_c=0.7 (or 70%). The values of the number of valence d holes are n_h=3.45 for Fe.[14] In Table I, the Fe magnetic moment values measured at different depths of the multilayer [Fig. 4(a)] are listed. The bulklike values for Fe spin moments are expected since the thickness of the Fe layers limits the sensibility to the interfacial Fe layers and for this reason we cannot probe a considerable reduction of the Fe spin moments, which is typical in the case of ultrathin films.

In the case of the *in situ* $Si(100)/[Fe(30\ Å)/Cr(27\ Å)]_{20}/Cr(30\ Å)$ sputtered multilayer, we reached several depths of the film by thinning the layer with Ar^+ ions. The intensities of the L_3 edges of the isotropic XAS for Fe and Cr are plotted in Fig. 8 as a function of the sputtered thickness of the film. The escape depth is also assumed to be around 60 Å. In a similar way the signal from Fe (Cr) increases (decreases) with increasing erosion depth of the sample, consistent with the amount of material present; the dotted line in Fig. 8 is just a guide for the eyes. XMCD measurements were taken after each one of the 21 sputtering cycles done on the sample, and this process was performed

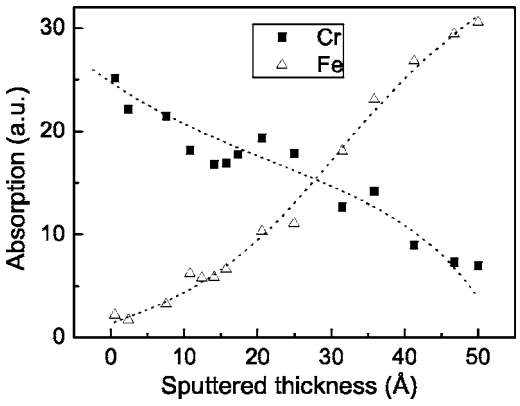

FIG. 8. X-ray absorption-depth profile for $[Fe(50\ Å)/Cr(27\ Å)]_{20}$ sputtered multilayer.

TABLE II. Spin and orbital magnetic moments for Fe in the *in situ* sputtered $[Fe(50\ Å)/Cr(27\ Å)]_{20}$ multilayer.

Sputtered thickness (Å)	m_s^{eff} (μ_B/atom)	m_l (μ_B/atom)
8	1.97	0.06
20	1.34	0.11
35	0.86	0.15
50	1.16	0.06

until a depth of about 50 Å was reached. The Fe magnetic moment values are listed in Table II. At the 8 Å of the eroded thickness, Fe m_s^{eff} is similar to the bulk value since at this depth, the sputtering process did not make substantial changes in the interfaces and it can be considered that the multilayer keeps its magnetic properties as prepared. However, we did not observe Cr dichroism at this stage, since the Cr thickness of the top Cr layer limits the interface sensitivity. For higher eroded thickness of the top Cr layer and assuming an ideal sputtering process (without surface and interface damage), it would be expected that the Fe m_s^{eff} would keep its value and a more expressive XMCD/isotropic XAS ratio for Cr was observed. However, in contrast, the opposite behavior was observed. The Fe m_s^{eff} decreased considerably and we observed a very noisy Cr dichroism. This result may be due to the interface broadening effect produced by the sputtering process that can lead to the formation of an Fe/Cr alloy with a weak or nonmagnetic order at the interface. This process leads to the decrease of the Cr XMCD signal, since the majority of the Cr atoms in the alloy are compensated, and besides very few Cr atoms from the layer can have contact with the ferromagnetic layer. In the case of the Fe m_s^{eff} the reduction is due to a higher interface (weak or nonmagnetic)/Fe bulk ratio. For the 35 Å eroded thickness a reduction of approximately 60% in the Fe m_s^{eff} compared to the bulk value was observed.

IV. SUMMARY AND CONCLUSIONS

In summary, we report a study of the interfacial regions of the $[Fe(50\ Å)/Cr(27\ Å)]_{20}$ multilayer by XMCD using two approaches. In the first approach, samples of the same type with different Cr capping layer thicknesses (30, 20, 10, and 5 Å) were produced and analyzed by XMCD. In the second method, the sample, as prepared, was eroded by several sputtering cycles. This sample composition was selected by preparing multilayers with different Cr layer thicknesses, which were characterized by magnetoresistance and magnetization measurements as well as by x-ray diffraction. Magnetoresistance measurements show that there is antiferromagnetic coupling between Fe layers when the Cr layer thickness is 27 Å.

The observation of Cr dichroism shows that there is an induced magnetic moment, which is antiparallel to the Fe and it was attributed to considerable hybridizations between Fe and Cr 3*d* orbitals at the interfaces. The Fe magnetic moments, in the nonsputtered samples, remained its bulk values due to the thickness of the layers. On the *in situ* sputtered sample we probed a considerable reduction of the Fe moments as the layers were eroded. This effect was attributed to

the very large intermixed interfaces caused by sputtering.

ACKNOWLEDGMENTS

This work was partially supported by FAPERJ (Pronex and Cientista do Estado), CT-Energ/CNPq, and Brazilian Synchrotron Light Source (LNLS) under Proposal Nos. D08A-SGM 2955 and D08A-SGM 5958. W.A. has a Ph.D. scholarship of CLAF-CNPq agreement. We acknowledge the LNLS staff for their prompt assistance at the SGM beamline. We are grateful to Professor W. Brewer (Frei Universitat Berlin) for a critical reading of the manuscript during his visit to CBPF supported by DAAD/CAPES collaboration program.

[1]S. S. Parkin, N. More, and K. P. Roche, Phys. Rev. Lett. **64**, 2304 (1990).
[2]P. Grünberg, R. Schreiber, Y. Pang, M. B. Brodsky, and H. Sowers, Phys. Rev. Lett. **57**, 2442 (1986).
[3]M. N. Baibich, J. M. Broto, A. Fert, F. Nguyen Van Dau, F. Petroff, P. Eitenne, G. Creuzet, A. Friederich, and J. Chazelas, Phys. Rev. Lett. **61**, 2472 (1988).
[4]D. Stoeffler and F. Gautier, Phys. Rev. B **44**, 10389 (1991).
[5]M. A. Tomaz, W. J. Antel, W. L. O'Brien, and G. R. Harp, Phys. Rev. B **55**, 3716 (1997).
[6]J. Meersschaut, J. Dekoster, R. Schad, P. Beliën, and M. Rots, Phys. Rev. Lett. **75**, 1638 (1995).
[7]B. T. Thole, P. Carra, F. Sette, and G. van der Laan, Appl. Phys. Lett. **68**, 1943 (1992).
[8]P. Carra, B. T. Thole, M. Alatarelli, and X. Wang, Phys. Rev. Lett. **70**, 694 (1993).
[9]S. Hofmann, Rep. Prog. Phys. **61**, 827 (1998).
[10]A. Ankudinov and J. J. Rehr, Phys. Rev. B **51**, 1282 (1995).
[11]T. Böske, W. Clemens, D. Schmittz, J. Kojnok, M. Shäfer, V. Cros, G. Y. Guo, and N. Eberhardt, Appl. Phys. A: Mater. Sci. Process. **61**, 119 (1995).
[12]C. T. Chen, Y. U. Idzerda, J. H. Lin, N. V. Smith, G. Meigs, E. Chaban, G. H. Ho, E. Pellegrin, and F. Sette, Phys. Rev. Lett. **75**, 152 (1995).
[13]F. Wilhelm, "Magnetic properties of ultrathin films, coupled trilayers and 3d/5d multilayers studied by x-ray magnetic circular dichroism," Ph.D. thesis, FU Berlin, 2000 (see http://www.dissertation.de/).
[14]A. Scherz, "Spin-dependent x-ray absorption spectroscopy of 3d transition metals: Systematics and applications," Ph.D. thesis, FU Berlin, 2003 (see http://www.dissertation.de/).
[15]R. Nakajima, J. Stör, and Y. U. Idzerda, Phys. Rev. B **59**, 6421 (1999).
[16]W. L. O'Brien, B. P. Toner, G. R. Harp, and S. S. P. Parkin, J. Appl. Phys. **76**, 6462 (1994).